Upper Tuolumne River Ecosystem Project:
Streambank Stability Study in Poopenaut Valley, Yosemite National Park, California

Technical Memorandum – Final

Prepared for
McBain & Trush
980 7th Street
Arcata, CA 94421

Prepared by
Stillwater Sciences
2855 Telegraph Ave., Suite 400
Berkeley, CA, 94705

February 2011

Stillwater Sciences

Suggested citation:
Stillwater Sciences. 2011. Technical memorandum on the upper Tuolumne River ecosystem project, streambank stability study in Poopenaut Valley, Yosemite National Park, California. Final. Prepared for McBain & Trush, Arcata, California.

Table of Contents

1 INTRODUCTION 1

1.1 Study Setting 1
1.2 Study Objectives 4

2 METHODS 5

2.1 Streambank Strength Parameters 5
2.2 Collection of Streambank Data 6
2.3 Bank Stability Modeling Setup 9
2.4 Bed Mobility Analysis 10

3 RESULTS 12

3.1 Field Measurements and Observations 12
3.1.1 Hydrographs of the Spring 2010 high-flow releases 12
3.1.2 Hydrologic parameters in the Southwest Tributary 12
3.1.3 Channel profiles and field observations 16
3.1.4 Bank material properties 20
3.2 Input Values and Results for Bank-Stability Modeling 20
3.2.1 Scenarios 1A and 1B: Spring 2010 high-flow releases 21
3.2.2 Scenarios 2A and 2B: threshold of failure identification 24
3.2.3 Scenarios 3A and 3B: pre-2010 drawdown rates 24
3.3 Bed Mobility Analysis Results 26

4 CONCLUSIONS AND RECOMMENDATIONS 28

5 REFERENCES 30

Tables

Table 1. Data types collected for the streambank stability study along the Southwest Tributary in Poopenaut Valley during the Spring 2010 high-flow releases 9
Table 2. Model inputs and factor of safety results for Scenarios 1A and 1B 23
Table 3. Model inputs and factor of safety results for Scenarios 2A and 2B 24
Table 4. Model inputs and factor of safety results for Scenarios 3A and 3B 25
Table 5. Bed mobility analysis results for four different median particle sizes and three different channel slopes 26

Figures

Figure 1. Site location and vicinity map of the streambank stability study in Poopenaut Valley, Yosemite National Park 2
Figure 2. Locations of the study site, valley tributaries, and NPS piezometer wells in Poopenaut Valley 3
Figure 3. Depiction of the forces affecting bank material shear strength in a streambank profile 5
Figure 4. Discharge in the Tuolumne River measured at the USGS stream gauging station below O'Shaughnessy Dam (USGS 11276500) during the Spring 2010 high-flow releases and the bank stability study 7
Figure 5. Comparison of channel cross-sections at the bank stability site representing pre- and post-study conditions 8
Figure 6. Plot of water surface elevation, or stage, in the river and tributaries, as measured at their respective stage recorders 11
Figure 7. Measured pore-water pressures at the six tensiometers installed in the top of the right bank of the Southwest Tributary at the bank stability study site 13
Figure 8. Plot of the recorded tributary stage and water table at the bank stability study site during the Spring 2010 high-flow releases 14
Figure 9. Plots of the recorded river stage and water table elevations at NPS measurement locations 15
Figure 10. Longitudinal profile of the Southwest Tributary, surveyed by NPS staff on 29 October 2007 16
Figure 11. Photos taken along the Southwest Tributary approximately 30 m upstream from the study site showing a before and after view of the channel where the only occurrence of bank failure was noted along the entire channel length 18
Figure 12. Photos taken of the bank stability study site on the Southwest Tributary before and after the high-flow releases 19
Figure 13. Plot showing the differentiation of the tributary stage into 31 steps for use in modeling Scenarios 1A and 1B 21
Figure 14. Plot of the tributary stage and estimated water table elevations during drawdown ramping rates as evaluated under Scenarios 3A and 3B 25
Figure 15. Plot of the bed mobility analysis results 27

1 INTRODUCTION

Operation of O'Shaughnessy Dam on the upper Tuolumne River has modified discharge and flooding patterns in the downstream river canyon compared with pre-dam conditions (RMC & McBain & Trush 2006). This modification, which is strongly pronounced during winter and spring, has specifically affected flooding dynamics in Poopenaut Valley—a broad alluvial valley situated along the upper Tuolumne River in Yosemite National Park (Stock et al. 2007). Concerns have recently been raised by the National Park Service (NPS) over the occurrence of bank failure and channel incision along the main tributary streams that traverse the valley floor. A hypothesis on the potential cause of the observed bank failures is that dam-induced reductions in flow following springtime water releases may be so rapid that streambank instability is induced as water levels in the valley drop quickly. The purpose of this study is to investigate the effects of the drawdown[1] ramping rates on the stability of the valley's tributary banks and to present recommendations for alternative drawdown rates that would minimize or avoid instability risk.

1.1 Study Setting

The study location is in Poopenaut Valley, described by Stock et al. (2007) as a broad, low-elevation (1,020 meters [3,350 ft] above sea level) valley positioned approximately 5 km (3.1 mi) downstream of O'Shaughnessy Dam—the dam responsible for regulating flow out of Hetch Hetchy Reservoir (Figure 1). The presence of the low valley within an otherwise narrow bedrock gorge makes the valley an important feature within Yosemite National Park from both an ecological and recreational-use perspective. The downstream end of the valley is constricted by the steep bedrock walls of the gorge, while shallow bedrock and local outcrops in the river channel act as natural grade controls maintaining the valley's elevation. Therefore, due to the hydraulic control caused by the constriction, this valley functions as a semi-closed basin during periods of high river discharge when flood waters back up within the valley, which causes fine sediment to deposit on the river floodplain that forms the valley floor (Stock et al. 2007).

Besides the river itself, there are three intermittent tributary channels that traverse the valley floor before joining the river at their respective confluences. These three streams are designated herein based on their relative locations in the valley—North Tributary, Southeast Tributary, and Southwest Tributary (Figure 2). These three stream channels are morphologically similar to one another—sinuous, somewhat incised, low-gradient channels that have cut through the alluvial substrates of the valley floor. The streams originate as steep mountain channels flowing down the canyon walls. A more detailed description of the tributary morphology on the valley floor is presented below.

For this study, we elected to focus our efforts on only one of these tributaries in order to efficiently capture bank-stability conditions that are representative of those occurring along the other tributary channels. The downstream end of the Southwest Tributary was chosen as the study site for three reasons: (1) its morphological features are representative of all three tributary channels, and any inferences drawn from its data will likely be applicable to the other two; (2) the stream is centrally positioned within an array of NPS groundwater monitoring wells (i.e., piezometers) that could provide useful hydrogeologic information for the area (see Figure 2); and (3) no river crossings were required for access.

[1] Drawdown is a term commonly used to describe the lowering water surface level in a reservoir. For this study, we have adopted the use of this term to describe the lowering of the river stage downstream of the dam caused when its outflow has been reduced.

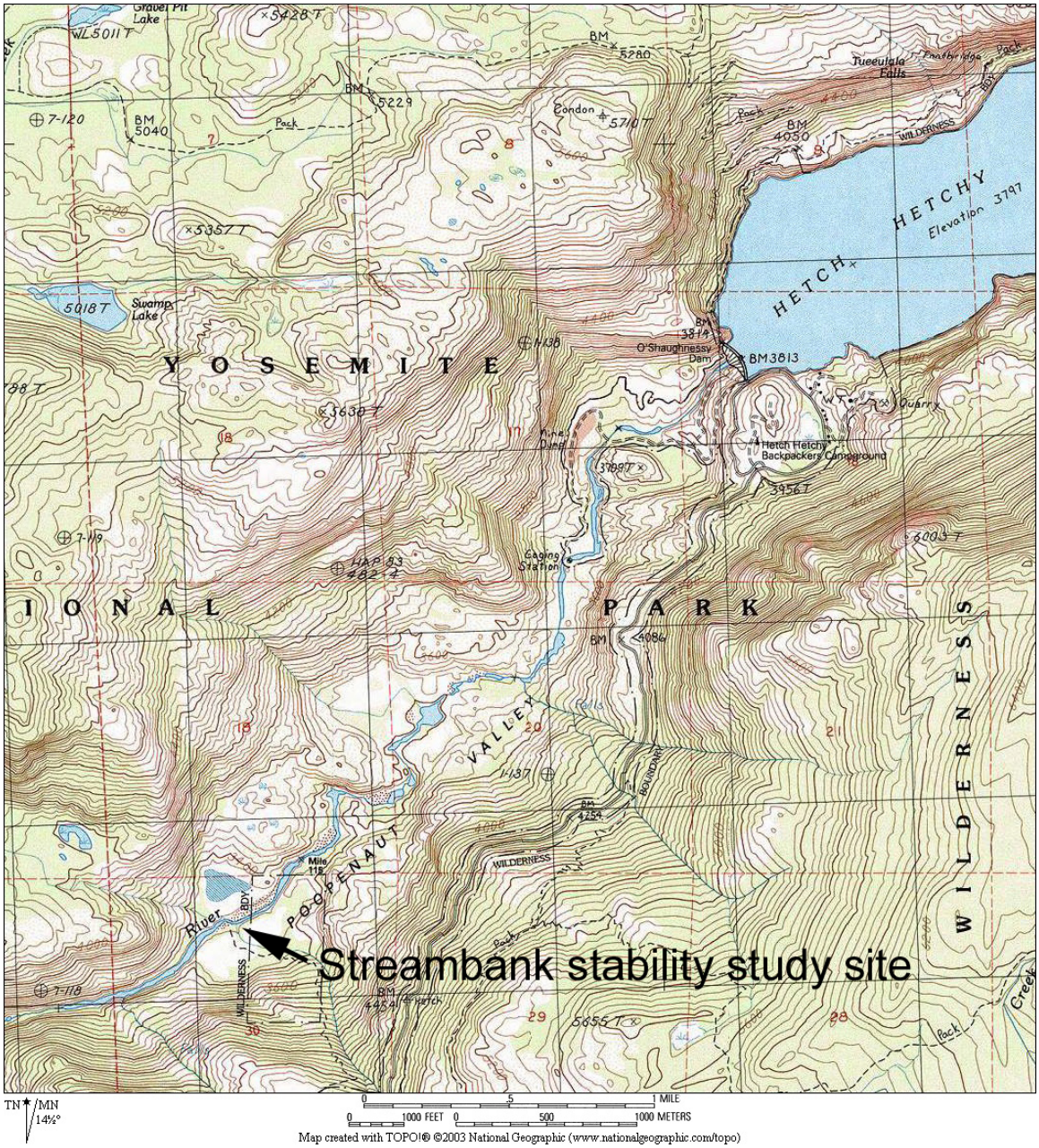

Figure 1. Site location and vicinity map of the streambank stability study in Poopenaut Valley, Yosemite National Park.

Figure 2. Locations of the study site, valley tributaries (shown as blue lines), and NPS piezometer wells (shown as red points) in Poopenaut Valley (after Stock et al. 2007). Stage recorders are also shown and designated as follows: Tuolumne River = "Upstream Stage" and "Downstream Stage"; Southwest Tributary = "SW Trib"; Southeast Tributary = "SE Trib"; and North Tributary = "North Trib".

1.2 Study Objectives

Drawdown-induced bank instability, often leading to mass failure of the bank, is a common phenomenon in alluvial streams around the world. Multiple academic and government-sponsored bank-stability studies have shown that when water-surface levels in stream channels drop much faster than do subsurface water levels within the adjacent streambank substrates (as expressed by the height of the groundwater table), the excess pore-water pressures[2] acting within the slowly draining substrates often cause these materials to become structurally unstable, resulting in mass failure of the streambanks (e.g., Fox et al. 2007, Rinaldi et al. 2004, Simon et al. 2000, Thorne 2000). Simon et al. (2000) states that "*Bank failures have been most commonly reported during the recessional period of stormflow and often can be represented analytically, as a saturated rapid drawdown condition.*" The authors list the conditions necessary to transform a stable bank into an unstable bank during periods of floodplain saturation (e.g., during periods of high flows and/or prolonged rainfall):

1. increase in soil bulk unit weight (i.e., increase in loading),
2. decrease or complete loss of matric suction[3] (i.e., reduction or loss of apparent cohesion),
3. generation of positive pore-water pressures (i.e., reduction or loss of frictional strength),
4. entrainment of in-situ and failed bank material at the bank toe, and
5. loss of confining pressure during recession of stormflow hydrographs.

Motivated by general concerns of bank failures in the valley's tributaries and by our own understanding of bank-stability mechanics, the objective of this study is to: (1) investigate the degree to which the dam-controlled drawdown rates following spring flow releases are inducing bank failure in the tributaries of Poopenaut Valley; and (2) assist others in developing recommendations for alternative drawdown ramping rates with less risk of induced bank failure. To accomplish these tasks, we continuously measured pore-water pressures and other key channel and bank properties during the Spring 2010 high-flow releases as they responded to the variations in streamflow and water level. The Spring 2010 high-flow releases were composed of a series of three high-flow pulses released from Hetch Hetchy Reservoir between May and June for the purpose of allowing this study to test the effects of different drawdown ramping rates on tributary bank stability. The data we collected during the flow releases were subsequently used in a bank-stability computer model (BSTEM) that evaluates the level of streambank stability at discrete moments in time during the monitored time period. The bank-stability model was further utilized to identify specific conditions not necessarily observed during this year's monitoring period that could potentially lead to unstable bank conditions (e.g., more rapid drawdown rates, loss of vegetation cover).

We additionally performed a cursory analysis of incipient motion of bedload particles in the study reach of the Southwest Tributary to gauge the potential for bed and bank toe scour during periods when tributary flows are high, but when the river flow is low. Although the analysis was not intended to determine if and when channel incision has been occurring, it does provide us with a first order estimate of erosion potential that can help to frame additional study questions of tributary bank failure mechanisms and general channel morphology trends, particularly as influenced by the hydrogeomorphic conditions of the Tuolumne River.

[2] Pore-water pressure is the static pressure exerted on surrounding soil particles within the pores of the subsurface materials by the weight of the overlying water.
[3] Matric suction occurs above the groundwater table and is the inverse of pore-water pressure—the negative pressure (i.e., suction) exerted by unsaturated water held in soil pores, and which adds effective cohesion to the surrounding granular materials.

2 METHODS

2.1 Streambank Strength Parameters

Data collection for this study concentrated on taking measurements of channel and bank material parameters that directly affect the strength of the bank materials. Bank strength is commonly characterized by the sum of five components: *cohesion* (the electro-chemical bonds between particles, normally significant for silt- and clay-sized soil grains), *internal friction* (inter-particle roughness across a potential plane of movement), *pore-water pressure* (which reduces internal friction by forcing grains apart), *matric suction* (the apparent cohesion caused by negative pore pressures in water in unsaturated soil), and the *normal load* (the weight of the bank acting perpendicular to the potential plane of movement, which tends to increase the interlocking of grains) (Figure 3).

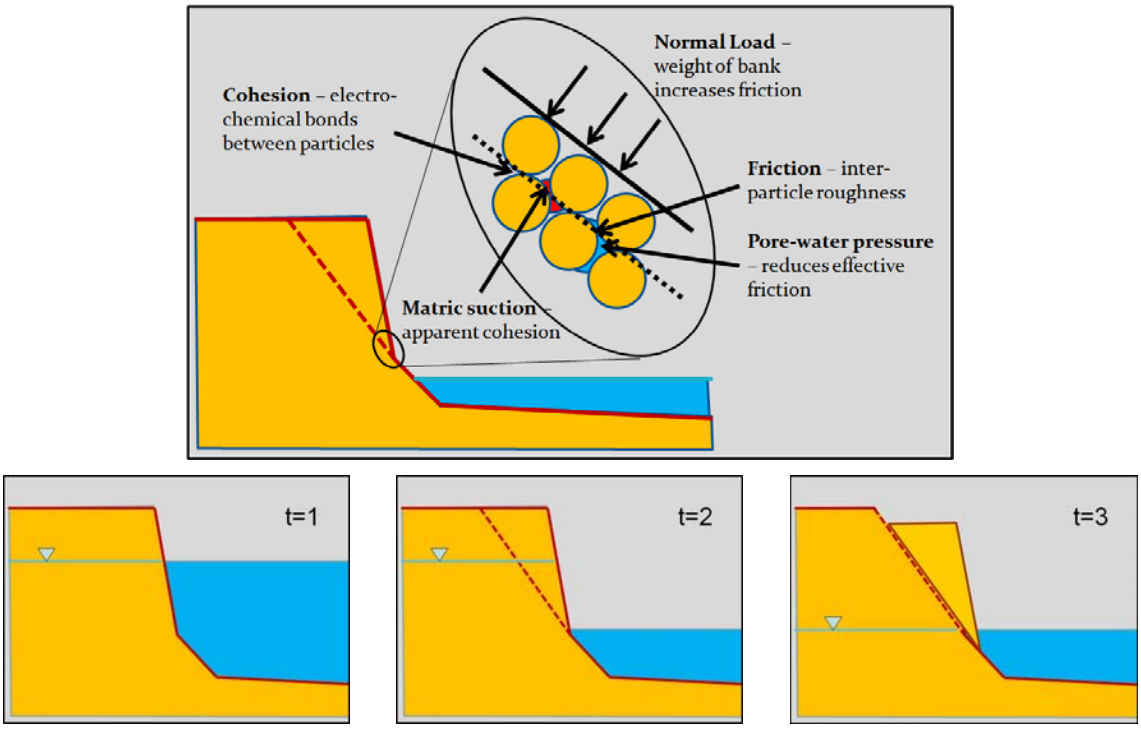

Figure 3. Depiction of the forces affecting bank material shear strength in a streambank profile (streamflow is into or out of the page) (after Langendoen et al. 1999). The upper illustration depicts the primary parameters affecting bank strength at the particle level, which in turn affects the entire bank mass (dotted line is a plane of potential movement, or the *failure plane*). The lower series of three illustrations together depict the progressive formation of a failure plane (dashed) during a period of drawdown (t=1 to t=2) when the lowering of the water table lags behind the falling of the stream stage (t=2: excess pore-water pressures within the bank materials and decreased confining pressures exerted by water in the channel), resulting in mass failure of the bank (t=3).

Mathematically, soil strength at a potential failure plane is defined in a more detailed manner as:

$$\tau_f = c' + (\sigma_n - \mu_a)\tan\varphi' + (\mu_a - \mu_w)\tan\varphi^b \quad (1)$$

where τ_f denotes soil shear strength (in units of stress, or a force per unit area), *c'* denotes effective cohesion of the soil, σ_n denotes the normal load of the overlying soil mass, μ_a denotes pore-air pressure acting on the failure plane (small, and so usually presumed equal to zero), φ' denotes the effective angle of internal friction associated with the normal stress state variable ($\sigma_n - \mu_a$; in degrees), μ_w denotes the pore-water pressure, and φ^b denotes the angle representing the increase in shear strength for an increase in matric suction ($\mu_a - \mu_w$; in degrees).

Ultimately, the degree of bank stability is dependent on the balance between the resisting forces (e.g., bank strength, cohesion, vegetation effects, normal load (or confining pressure), internal friction angle) and the driving forces (e.g., bank slope, degree of saturation, pore-water pressure, weight of the bank). The ratio of these forces represents the factor of safety, F_s, which is defined simply as:

$$F_s = \tau_f \frac{L}{S} = \textit{Resisting Forces / Driving Forces} \quad (2)$$

where *S* denotes the shear force at the base of the failure block and *L* denotes the length of the inclined slip surface, or failure plane (Langendoen et al. 1999, Simon et al. 2009).

This relationship is derived from basic engineering principles whereby a stable condition is maintained provided that the resisting forces are greater than the driving forces. Thus, bank stability is achieved with $F_s > 1$ and bank instability is presumed to occur when $F_s < 1$. For this study, we have adopted the standards recommended by the U.S. Department of Agriculture's National Sediment Laboratory (USDA-NSL), whereby an "unstable" condition is reached when $F_s < 1$ and a "conditionally stable" condition exists when $1 < F_s < 1.3$ (Simon et al. 2009). Stable conditions are achieved when $F_s > 1.3$, although the USDA-NSL note that a higher standard (e.g., $F_s > 1.5$) should be considered if a given project requires one. For the purposes of this study, we believe the 1.3 standard is sufficient here as higher standards are typically reserved for engineering design work.

2.2 Collection of Streambank Data

The Spring 2010 high-flow releases provided an opportunity to monitor streambank conditions in Poopenaut Valley during three periods of valley inundation and variable drawdown ramping rates in a two-month period (Figure 4). Data collection was focused along the lower reach of the Southwest Tributary, approximately 25 meters upstream from the stream's confluence with the Tuolumne River (Figure 2). The channel here is incised, having steep, high (4 m) banks as it cuts through the river's natural levees (Figure 5). Collection of pore-water pressure, bank profile, tributary stage, and bank-material properties data occurred along a transect trending perpendicular across the tributary channel. This cross-section was analyzed with the bank-stability model for this study (see below). The specific data types collected and analyzed during the study are listed and explained in Table 1.

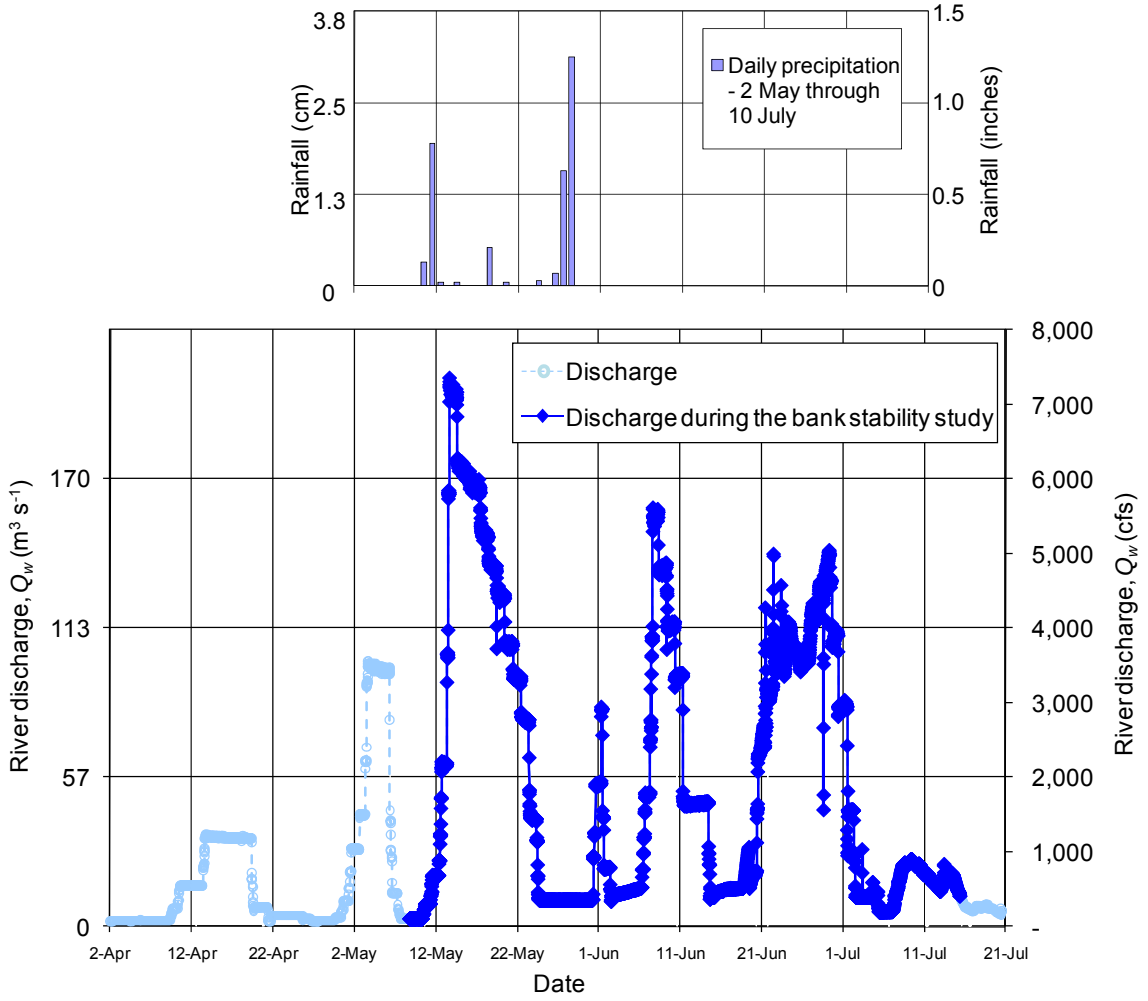

Figure 4. Discharge in the Tuolumne River measured at the USGS stream gauging station below O'Shaughnessy Dam (USGS 11276500) during the Spring 2010 high-flow releases and the bank stability study (bottom plot). Discharge computed every 15 minutes. Precipitation recorded as rainfall at the O'Shaughnessy Dam gauge (station OSH) between 2 May and 10 July, 2010 (top plot).

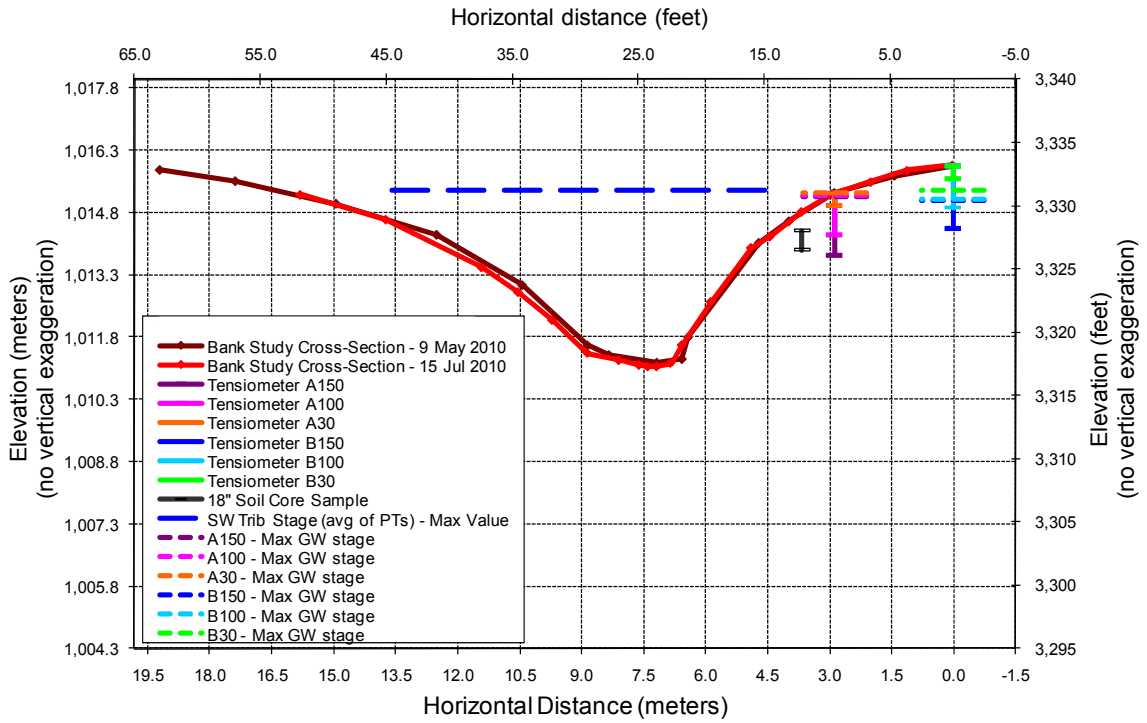

Figure 5. Comparison of channel cross-sections at the bank stability site representing pre- and post-study conditions (view looking downstream). The comparison reveals that no changes in the cross-section profile occurred during the Spring 2010 high-flow releases. The small deviation visible between the two cross-sections is due to normal survey variability due to differences in specific rod placement between the two surveys. The locations of the six tensiometers and the soil core sample are also shown for reference. The maximum flood stage and groundwater level in the stream channel are also shown (dashed blue line).

Data collection was conducted by Stillwater Sciences staff and assisted by NPS staff. The tensiometer equipment[4] was loaned by the Watershed Physical Processes Unit of the USDA's National Sedimentation Laboratory in Oxford, Mississippi. The six tensiometers were installed in two rows along the top of the right bank, spaced apart by 3 m. Each row consisted of a 0.3-, 1.0-, and 1.5-m-long tensiometer spaced 1 m apart. The front row (A row) was closest to the stream channel. The back (B) row served as a redundant measure in case any of the equally sized tensiometers in the A row malfunctioned during the study (which did not occur).

Analysis of the hydraulic properties of the bank materials were conducted by Stillwater Sciences staff in the soils laboratory of the Geosciences Department of San Francisco State University. The measurement of porosity was attained volumetrically and gravimetrically using a porosimeter, and the measurements of permeability and hydraulic conductivity were achieved using a constant head permeameter. Although neither the porosity nor the hydraulic conductivity values measured were subsequently used in the bank stability model (see below), they nevertheless provided additional, useful information on how efficiently surface water infiltrates into and groundwater drains from the bank materials[5]. Finally, soil strength analysis (cohesion and friction angle) was performed by a certified, third-party geotechnical laboratory.

[4] A tensiometer is a device installed in the ground that records pore-water pressures (and matric suction).
[5] Note: the next version of the bank stability model software will include a groundwater module that will utilize porosity and hydraulic conductivity values (A. Simon, pers. comm., 2010).

Table 1. Data types collected for the streambank stability study along the Southwest Tributary in Poopenaut Valley during the Spring 2010 high-flow releases.

Data type collected at the study site (or in the vicinity)	Frequency of data collection	Manner of data collection
Cross-section profile of channel	Before and after flow releases	Elevation survey of the study cross-section taken with auto-level survey equipment
Local longitudinal profile of the tributary channel bed		
Pore-water pressures (μ_w) and matric suction ($\psi = \mu_a - \mu_w$) (and groundwater elevations)	Continuous (1-hr increments)	Installed six (6) tensiometers in the top of the right bank along the study cross-section
Water-surface elevation	Continuous (1-hr increments)	Installed two (2) pressure transducers on the stream bed immediately upstream and downstream of the study cross-section
Discharge in the Tuolumne River (Q_w)	Continuous (15-min increments)	USGS stream gauging station 11276500
Precipitation at O'Shaughnessy Dam	Daily totals	SFPUC Hetch Hetchy Water and Power (station OSH) and Department of Water Resources – California Data Exchange Center (station HTH)
Bank material properties: porosity (n), permeability, hydraulic conductivity (k), and soil strength (cohesion [c']and friction angle [φ'])	Single sample of bank substrate taken at the end of the study	Soil core sample taken at 1 meter below grade surface at the top of the right bank; soil properties analyzed in the laboratory
Qualitative observations and photographs of the stream channel and floodplain morphology, bank soils, and vegetation effects	Before and after flow releases, supplemented with NPS staff observations during the flow releases	Observations made and photographs taken along the entire Southwest Tributary in the valley, including the valley floor itself

2.3 Bank Stability Modeling Setup

An established, peer-reviewed computer software model was utilized to augment the field observations by calculating the degree of bank stability (or Factor of Safety, F_s) at various moments of the Spring 2010 high-flow releases using the field measured data. The model used was the Bank-Stability and Toe Erosion Model (BSTEM; version 5.2), developed by the USDA-NSL for the intended purpose of analyzing bank failure mechanisms and the processes that influence them (Simon et al. 2009). The model was also utilized to investigate the specific factors that trigger bank failure during other drawdown scenarios that were not specifically implemented as part of the Spring 2010 high-flow releases.

We modeled three pairs of scenarios:

Scenario 1A: Spring 2010 high-flow releases with vegetation – using the field-collected data, we divided the flow release hydrographs into 31 steps at key inflection points of the hydrographs; includes added cohesion from plant roots

Scenario 1B: Spring 2010 high-flow releases without vegetation – same conditions as Scenario 1A, but without the added cohesion from roots

Scenario 2A: Threshold of bank failure with vegetation – focusing on a hypothetical hydrograph not actually monitored during the flow releases, we modeled several extreme cases of drawdown, whereby the tributary stage was progressively lower than the adjacent groundwater table to identify the conditions under which failure could potentially occur; includes the added cohesion from vegetation

Scenario 2B: Threshold of bank failure without vegetation – same conditions as Scenario 2A, but without the added cohesion from vegetation

Scenario 3A: Standard drawdown ramping rates with vegetation – using approximate drawdown rates that had occurred in years prior to 2010 (i.e., 50% reduction in flow every four hours), we modeled several moments along this representative hydrograph to determine whether the more rapid drawdown periods of years past could potentially induce bank failure; includes the added cohesion from vegetation

Scenario 3B: Standard drawdown ramping rates without vegetation – same conditions as Scenario 3A, but without the added cohesion from vegetation

The purpose of evaluating the "B" scenarios was to examine the effects of vegetation on the overall stability of the modeled bank profile. In the valley, vegetation can be denuded from the bank surfaces by high scouring flows in the tributaries and by wildfire[6].

2.4 Bed Mobility Analysis

Our analysis of incipient motion of sediment particles on the channel bed of our study reach involved estimating a threshold stream stage, or flow depth, required to initiate entrainment of individual particles of a given size. As stated previously, this analysis is intended to help gauge the difference between bed stability and bed mobility for the purpose of assessing the potential for erosion of the channel bed when high flows are being conveyed through the tributaries, but when the river flows are low (i.e., free flow to the tributary mouth). Incipient motion is expected to occur when the boundary shear stress exerted on a given particle during a certain discharge exceeds the critical shear stress for the channel cross section. If the bed is estimated to be mobile during certain flows, it can be deduced that the channel could be vulnerable to certain morphologic changes, such as incision, which could further destabilize (i.e., undermine) the adjacent streambanks. The bank stability model, BSTEM, has the ability to model bank toe scour, but not channel bed incision(or incipient motion of bed particles. Therefore, for this analysis, we utilized the Shields equation to estimate the threshold conditions necessary to initiate bedload transport of certain particle sizes:

$$\tau^*_{crit} = \frac{\tau_{crit}}{(\rho_{sed} - \rho_{water})gD_{50}} \quad (3)$$

where τ^*_{crit} is the dimensionless critical shear stress, or Shields number (assumed to equal 0.047 for D_{50} of the gravel bed particles), ρ_{sed} is the density of the sediment particle (assumed to equal 2.65 grams per cubic centimeter [g/cm^3]), ρ_{water} is the water density (1.0 g/cm^3), g is gravitational

[6] Over the past century, there have been three wildfires recorded in the valley—1968 (Poopenaut Fire), 1953 (Hetch Hetchy Fire), and 1996 (Ackerson Fire; largest event)—based on a query of the CDF FRAP database (2010).

acceleration (981 cm/s^2), D_{50} is the median bed material particle size, and τ_{crit} is the critical boundary shear stress (force per unit area), which is calculated as follows:

$$\tau_{crit} = \rho_{water} g R_h S \quad (4)$$

where R_h is the hydraulic radius (cross-sectional area divided by the wetted perimeter of the channel) and S is the slope of the channel.

For this analysis, we calculated the critical depth of flow necessary to mobilize four different particle sizes that are representative of median bed material sizes present at our bank stability study site reach: 2, 10, 20, and 32 mm. Because channel slopes also vary along the length of the tributary's course through the valley, we additionally considered three representative slopes in our calculations: 0.005, 0.0125, and 0.04. The calculations utilized the following field-collected data: channel cross-section and longitudinal profile (surveyed by NPS and McBain & Trush staff in October 2007. Stage data from the water stage recorder (October 2007-July 2010) located farther up the tributary was adjusted to our study site and used in our analysis to determine whether bed mobilization, and possibly channel incision, could have occurred in recent years when tributary flow was relatively high, but when the river flow was low (Figure 6). Accordingly, comparisons of measured stage and our calculated critical flow depths associated with the three bed slope scenarios and the four different bed particle size were not made during the spring high flows of 2009 or 2010.

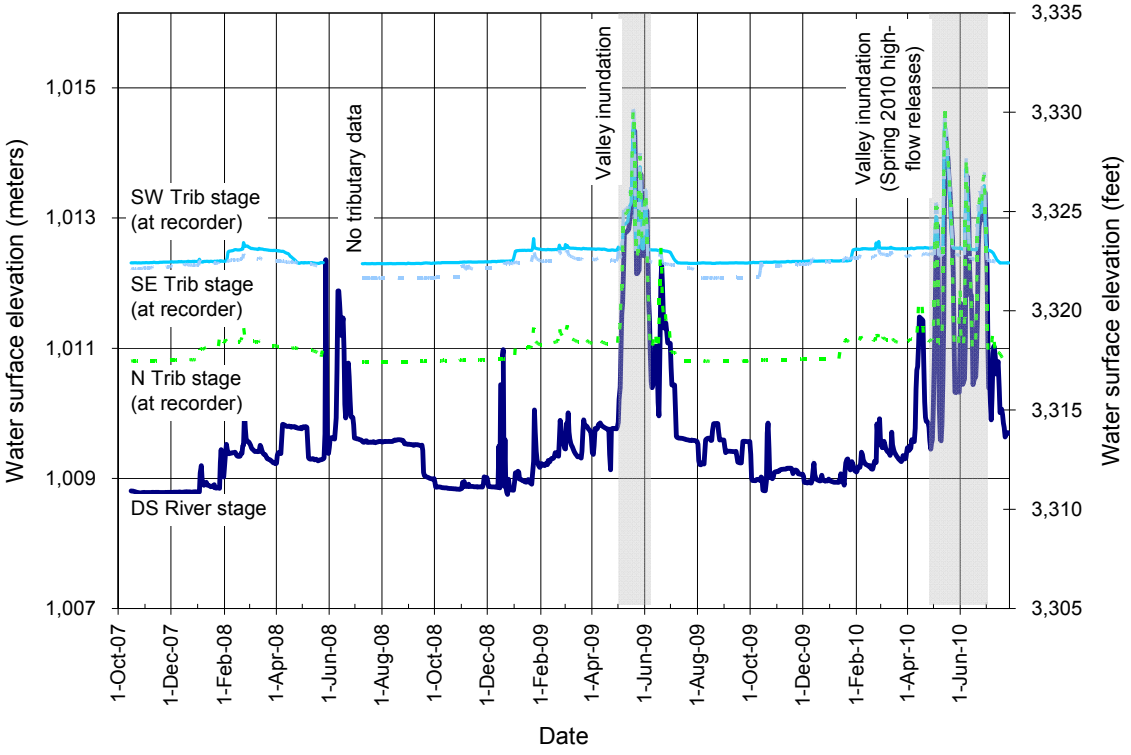

Figure 6. Plot of water surface elevation, or stage, in the river and tributaries, as measured at their respective stage recorders (see Figure 2 for locations of stage recorders). [Data source: preliminary, unpublished NPS data collected since October 2007.]

3 RESULTS

3.1 Field Measurements and Observations

3.1.1 Hydrographs of the Spring 2010 high-flow releases

The Spring 2010 high-flow releases consisted of a series of three high flow pulses, each with their own unique characteristics, or hydrograph shape, as defined by their peak magnitudes, total duration, and drawdown ramping rates. It is the third characteristic that we were most interested in for this study, as the time it takes for the high flows to subside directly affects drawdown rates in the river, on the valley floor, in the valley tributary channels, and in the valley's subsurface (i.e., groundwater table). Discharge in the Tuolumne River downstream of O'Shaugnessy Dam during the Spring 2010 high-flow releases, along with daily rainfall totals at the dam, are presented in Figure 4 above.

3.1.2 Hydrologic parameters in the Southwest Tributary

The six tensiometers successfully recorded pore-water pressures at their respective locations and depths in the right bank of the study site throughout the flow releases (Figure 7). Trends in these data reflect periods of saturation and drying as the water table rose and fell in accord with the flooding of the valley. The deeper portions of the bank experienced greater pore-water pressures, while the shallower portions experienced lower pore-water pressures for a given moment in time. However, one exception to this trend was during late May when rainfall partially saturated the shallow depths of the bank top, momentarily causing the shallower tensiometers to record relatively higher pore-water pressures than was recorded by the deeper tensiometers.

The water-surface elevations in the tributary channel, as recorded by the two pressure transducers anchored to the stream bed at the study site, fluctuated in accord with the flood pulses in the river (Figure 8). The two brief rainfall events on May 10–11 and 27–28 did not result in detectable streamflow in the channel and no other flow events unique to the valley's tributaries occurred during the two-month experimental flow release. Therefore, inundation in the Southwest Tributary was wholly influenced by the dam-controlled flows in the river.

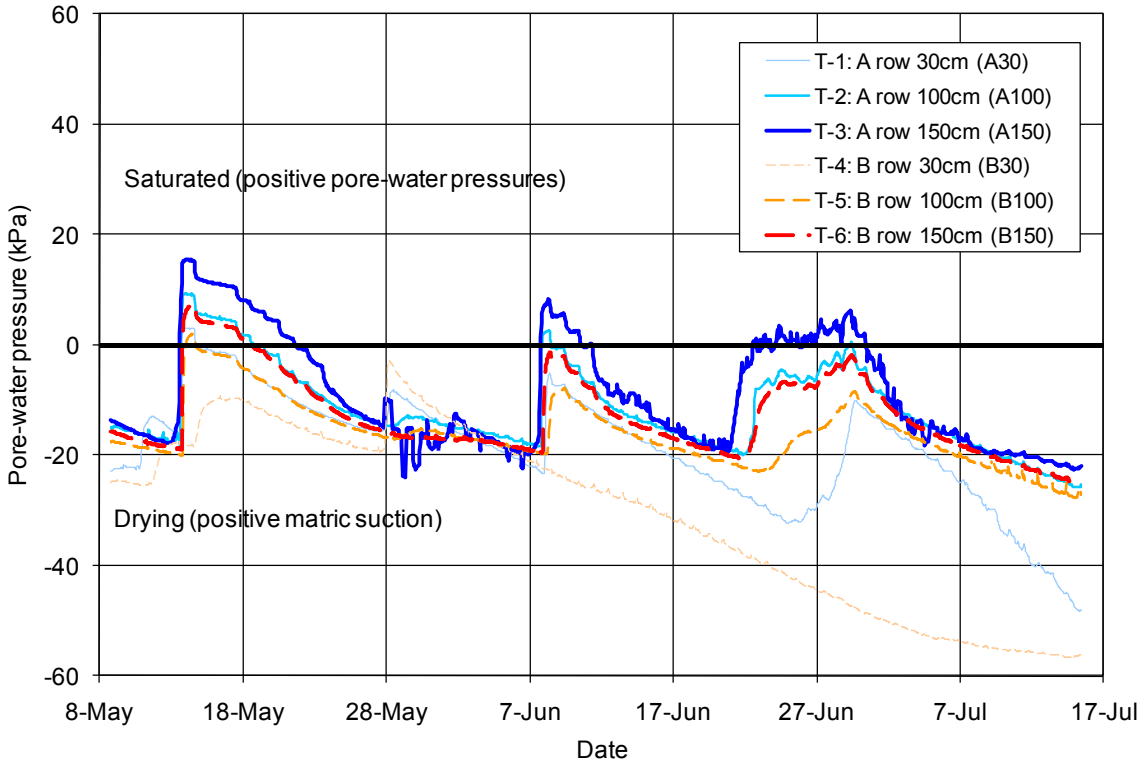

Figure 7. Measured pore-water pressures at the six tensiometers installed in the top of the right bank of the Southwest Tributary at the bank stability study site. Values greater than zero indicate saturated conditions during valley inundation, while values less than zero indicate drying (i.e., positive matic suction) conditions during drawdown. The deeper tensiometers experienced the greatest pore-water pressures.

Because the tensiometers are sensitive to the degree of saturation in the bank materials, their data provides a decent record of the fluctuations in the water table. When the bottom of a tensiometer (location of its pressure sensor) is below the water table, it effectively functions the same as a piezometer where an accurate reading of the water table elevation is recorded. When the water table drops below the bottom of a tensiometer, the data recorded characterizes the drying of the bank materials, or the matric suction, at the depth of the tensiometer's sensor. The matric suction values can closely, but not exactly, represent the elevation of the falling water table. We have used the data from the deepest tensiometer (A150) to represent groundwater-table elevations when the water table was above the bottom of the tensiometer (at elevation 1,013.5 m [3,325 ft]), which generally correspond well with the water-surface elevations in the tributary channel (Figure 8). Within this upper half of the bank, the water table kept pace with the fluctuating tributary stage, indicating that the flood waters easily infiltrated and drained from the bank and floodplain materials (i.e., high hydraulic conductivity; see below).

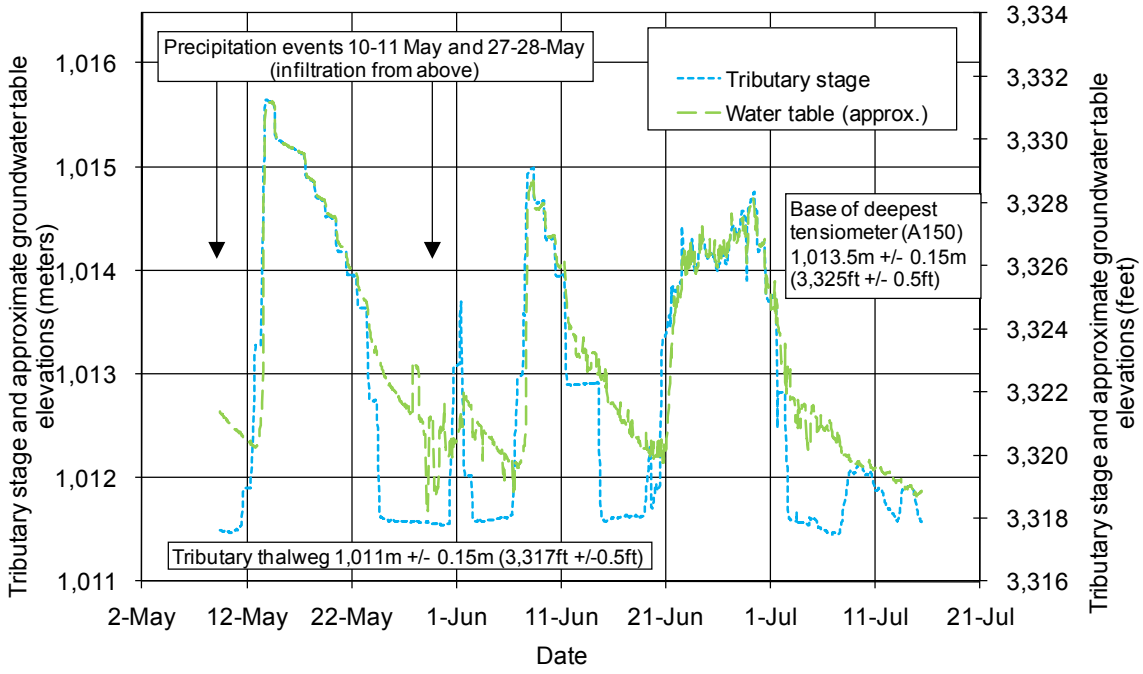

Figure 8. Plot of the recorded tributary stage and approximate water table elevations at the bank-stability study site during the Spring 2010 high-flow releases. As shown, the estimated water table generally kept pace with the changing water-surface elevations in the stream channel during the rising and recession periods of the flood peaks when above 1,013.5 m (3,325 ft). Below this elevation, the estimated water table deviates from the falling tributary stage giving the appearance that groundwater drained at relatively slower rates when positioned within the lower half of the bank profile.

The trend in the measured matric suction values during the drawdown periods suggest that the rates of the draining groundwater slowed when the tributary stage and water table dropped below 1,013.5 m (3,325 ft), which coincides with the elevation of the bottom of the deepest tensiometer (A150). However, because these values only represent matric suction and do not accurately represent the water table elevation, it is unclear whether these slower draining rates are real. Review of river stage and water table measurements recorded elsewhere in the valley during the high-flow releases was therefore undertaken to investigate whether the surface water infiltration and groundwater draining patterns exhibited at the bank stability study site were unique. River stage data from the NPS' upper and lower stage recorders were compared with water table elevation data collected at Wells 8 and 3, respectively (see Figure 2 for their locations). As clearly captured in the data presented in Figure 9[7], the water table at these locations kept close pace with the nearby river stage (and tributary stage for Well 8) when the water table was above 1,012.5 m (3,322 ft), but began to deviate from the river stage (i.e., draining at a slower rate) below this elevation during the drawdown periods. Therefore, the infiltration and draining patterns measured at our bank stability site and at the NPS' wells and stage recorders are very similar, which, taken together, indicate the following: (1) high flows from the river quickly infiltrated the tributary banks and valley substrates; (2) groundwater quickly drained from the saturated banks during the drawdown periods when the water table was above a "threshold" elevation of approximately 1,013 m (3,323 ft); and (3) groundwater drained more slowly and the water table became progressively higher relative to the falling river and tributary stages when the water table was below this threshold elevation.

[7] These are preliminary, unpublished data from the NPS and may be subject to further refinement.

a)

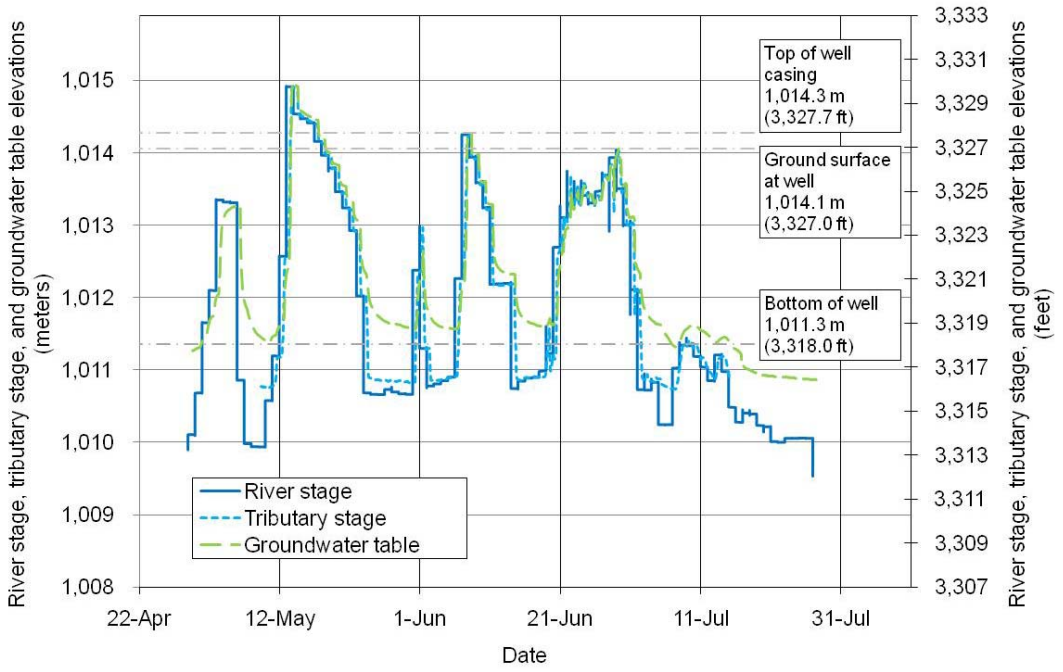

b)

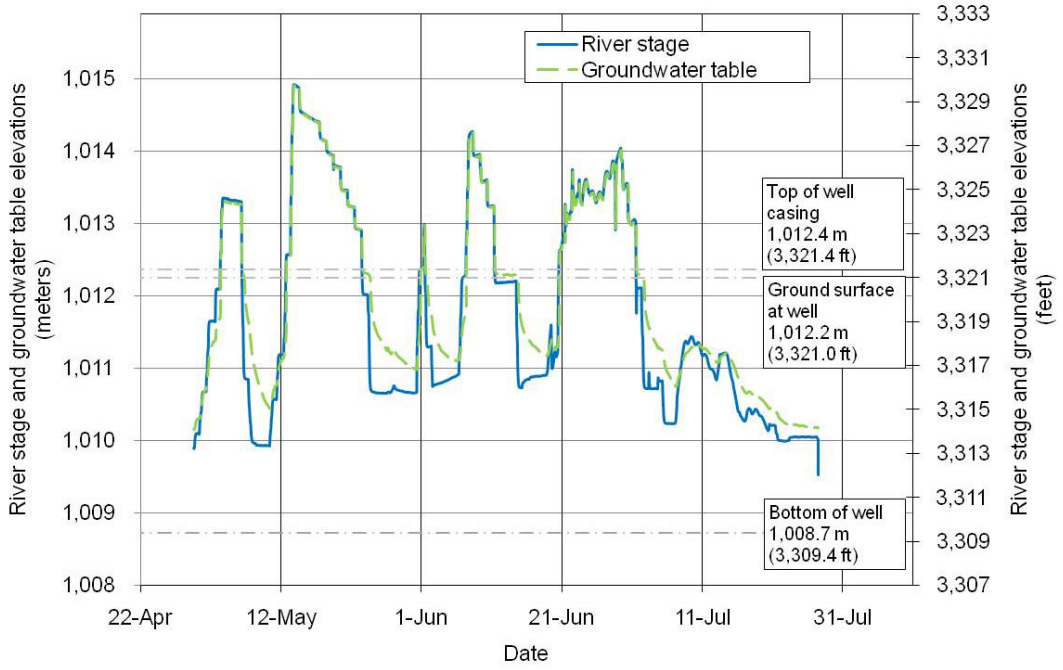

Figure 9. Plots of the recorded river stage and water table elevations at NPS measurement locations: upper stage recorder and Well 8 (a) and lower stage recorder and Well 3 (b). The stage in the Southwest Tributary is also shown in comparison to the upper river stage recorder data (a). Elevations of the two wells' top of casing, ground surface, and bottom are also shown for reference. As depicted in both (a) and (b), the water table generally kept pace with the changing river stage (and tributary stage near Well 8) during the rising and recession periods of the inundation peaks when above 1,012.5 m (3,322 ft). The water table deviated from the falling river stage indicating that the groundwater drained at a relatively slower rate when below this threshold elevation. [Data source: preliminary, unpublished NPS data collected during the Spring 2010 high-flow releases.]

3.1.3 Channel profiles and field observations

The Southwest Tributary is characterized by a moderately sinuous, low-gradient alluvial channel with fine sandy loam banks and a sandy gravel bed. Although sampling of the bed materials for analysis for their size distribution was not conducted, the median grain size (D_{50}) was visually estimated to be approximately 4 mm in diameter, but patches of coarser particles were noted throughout. The channel exhibits a subtle bar-pool morphology that transitions to a more plane-bedded, incised channel closer to the confluence with the river. The thalweg gradient along the lowermost 275 m of the channel, as surveyed in 2007 by NPS staff, is approximately 1% (Figure 10). The degree of channel incision increases with downstream distance, particularly as the channel cuts through a natural levee deposited upon the river's left bank (see the small square and circle symbols in Figure 10 representing the elevation of the top of the left and right banks). The tributary channel is incised, with steep banks reaching up to 4 m above the channel bed (Figure 5). The bank profile is convex, rather than being vertical with a well-defined edge at the top of the bank. Vegetation coverage also increases with downstream distance, supporting riparian species such as willows, cottonwoods, incense cedars, and black oaks that grow on the floodplain and bank surfaces. Throughout the valley and in the channels, there is a dense herbaceous coverage which likely provides yet another level of protection to the streambanks, by shielding the banks from excess shear stresses during high tributary flows and by providing additional cohesion to the bank materials (Figure 11).

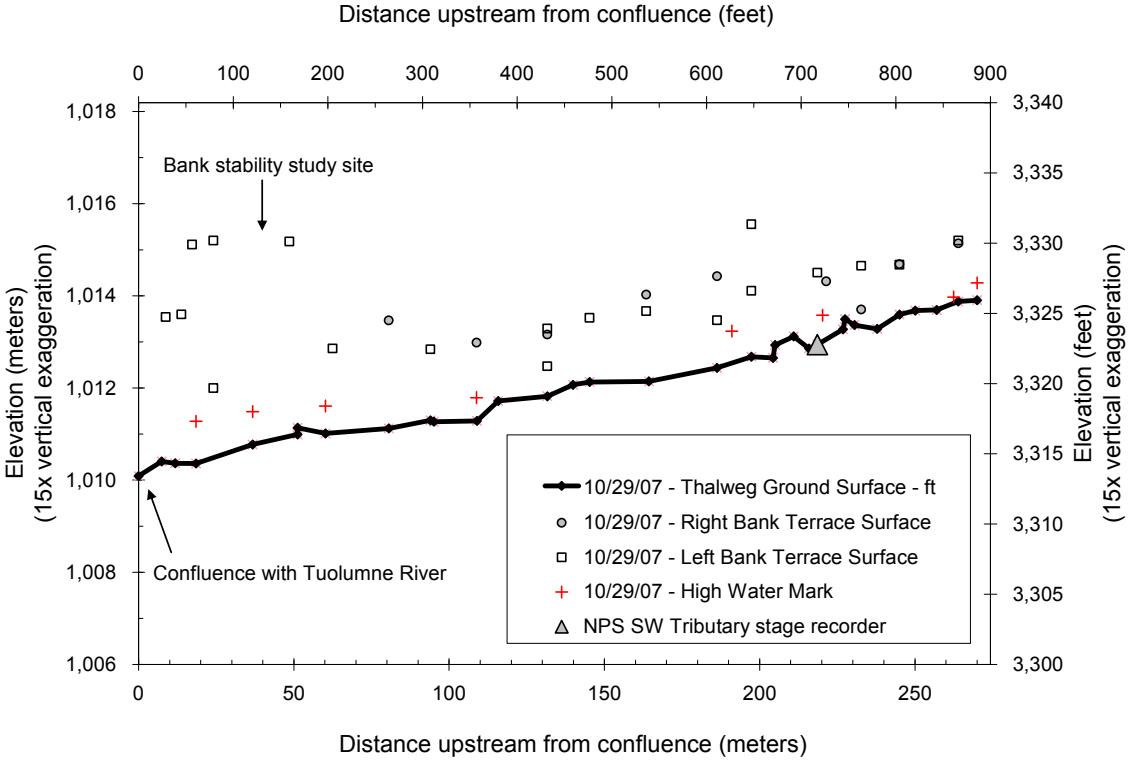

Figure 9. Longitudinal profile of the Southwest Tributary showing the bank stability study site, the NPS stage recorder locations, the elevations of the right and left bank terraces, and the high water marks as observed by the surveyors (29 October 2007) based on geomorphic indicators.

Overall, there was a single observed occurrence of bank failure along the entire ~250 m length of the Southwest Tributary during the study period (Figure 11). This single failure represents approximately 0.25% of the total linear distance of both banks combined. The failure is characterized as a rotational slide of a relatively small mass (~1 m^3) that occurred after the formation of a failure plane in the subsurface of the bank. This mass fell directly upon the bank toe and appeared to retain most of its original volume. No failure occurred at the study site based on field observations and on repeat surveys of the channel's cross-section (Figures 5 and 12). Further inspection of the banks did not reveal any signs indicative of bank failure, such as tension cracks or groundwater seepage (piping). Herbaceous and shrub vegetation coverage on the floodplain, banks, and even on the channel bed increased considerably during the study period, which is likely a normal phenomena in late spring as vegetation growth is induced by seasonal factors rather than by any influences from the high-flow releases implemented this year. In the other two valley tributaries, observations made by NPS staff during and following the high flow releases did not note any apparent occurrences of bank failure (J. Roche, pers. comm., 2010).

New deposits of very fine sediments (silts and fine sand) were noted at various points along the channel bed, but no deposits of coarse sediments (coarse sands and gravels) were noted. The fine sediment deposits essentially formed a veneer over coarser sediments. It did not appear that any coarse sediment patches that were noted prior to the high flow releases changed form or location during the study, indicating that bedload transport was minimal, or absent all together. There was also no evidence of bank toe erosion in the channel. Taken together, these findings indicate that shear stresses were modestly low when the river's high flows were rising and falling in the tributary channel.

Figure 11. Photos taken along the Southwest Tributary approximately 30 m upstream from the study site showing a before and after view of the channel where the only occurrence of bank failure was noted along the entire channel length.

Figure 12. Photos taken of the bank stability study site on the Southwest Tributary before and after the high-flow releases. Note the absence of bank failure and the increase in herbaceous vegetation coverage on the bank surface.

3.1.4 Bank material properties

The streambanks are uniformly composed of a very fine sandy loam with no distinguishable stratigraphy from the bank top to the bank toe. We noted during the installation of the tensiometers that the soil was very loose and easily compacted with minimal pressure applied, which likely explains the convex, or rounded, profile of the bank as the soil materials lack the adequate degree of cohesion to maintain a more vertical profile. Roots from the vegetation growing on the top of the bank (e.g., *Prunus virginiana*) and grasses on the bank top and slope were observed to depth (~1.5 m below grade surface) and are assumed to continue to greater depths. Soil boring logs recorded by the NPS staff during the installation of three of their piezometer wells in the vicinity of our study site noted the following (see Figure 2):

- Well 9 – 0 to 3.80 m (1,015.3–1,011.5 m in elev.): sandy loam
- Well 8 – 0 to 2.15 m (1,014.1–1,011.9 m in elev.): sandy loam, 2.15 to 2.30 m (1,011.9–1,011.8 m in elev.): rocky lens, 2.30 to 2.72 m (1,011.8–1,011.3 m in elev.): coarse sand with larger rocks and gravel (see Figure 8a)
- Well 6 – 0 to 0.10 m (1,015.8–1,015.7 m in elev.): sandy loam, 0.10 to 2.20 m (1,015.7–1,013.6 m in elev.): sandy loam grading to sandier, 2.20 to 3.80 m (1,013.6–1,012.0 m in elev.): sandier (less organics)

These soil logs capture the depth of our study site, which was approximately 4 m with a channel thalweg elevation of 1,011 m.

Based on laboratory analysis, the bank materials have a porosity of about 30%, a value that falls within the range for fine sand (26–53%; Domenico and Schwartz 1998). The measured hydraulic conductivity value of 0.0004 cm/s is consistent with semi-pervious materials composed of unconsolidated, very fine sandy loam (0.01–0.00001 cm/s; Bear 1988). The soil strength measurements yielded the following values: effective stress cohesion (c') = 7.2 kPa and effective stress of internal friction (φ') = 29.5°. The cohesion value indicates, understandably, that the materials themselves possess very low internal shear strength without the added strength provided by water surface tension when partially saturated (Sarsby 2000) and by vegetation.

3.2 Input Values and Results for Bank-Stability Modeling

In all modeling scenarios, we imported the bank profile, channel slope, and material properties, which were assumed to remain constant throughout the study period. Vegetation effects were incorporated in the model (for the "A" Scenarios) using the RipRoot module (Pollen and Simon 2005), where the applied root cohesion was based on "5-year old, 100% wet meadow vegetation". The added cohesion from this vegetation type and assemblage was about 3 kPa, or nearly half of the laboratory-analyzed effective stress cohesion of the bank soils.

In all scenarios, the bank was differentiated into five horizontal layers, per the requirements of the model. Because soil properties were not analyzed for each of these layers, the effective cohesion, cohesion from vegetation, and effective internal friction values were repeated in each layer, which is an appropriate approach given the observed relative homogeneity of the bank soils.

After all data had been entered for each modeling scenario and each scenario's individual time step, the model produced a factor of safety value for that particular step (Equation 2).

3.2.1 Scenarios 1A and 1B: Spring 2010 high-flow releases

Incorporating the continuously recorded data from the two-month-long study into BSTEM was infeasible due to the sheer volume of data collected (over 1,600 pairs of data). To better manage this large dataset yet still effectively model the stability conditions during the study period, we differentiated the flood hydrographs into 31 steps, where a step was assigned when there was a 1-m change in tributary stage or the stage reversed direction, such as at a flood peak. Thus, periods of the flow releases having dramatic changes (e.g., period of inundation) had several close-together steps, while periods having minimal changes (e.g., low flow between the inundation peaks) had relatively few steps (Figure 13). The location of the steps, or nodes as shown in Figure 13, ultimately makes no difference on the model's computations because the model is simply evaluating the conditions present at that particular moment in time and has no consideration of conditions that occurred prior to or following that moment. That is, all nodes evaluated by the model are computational locations that together capture the range of head differentials that occurred over the hydrographs and that changing the node locations or their spacing would not change the computational results.

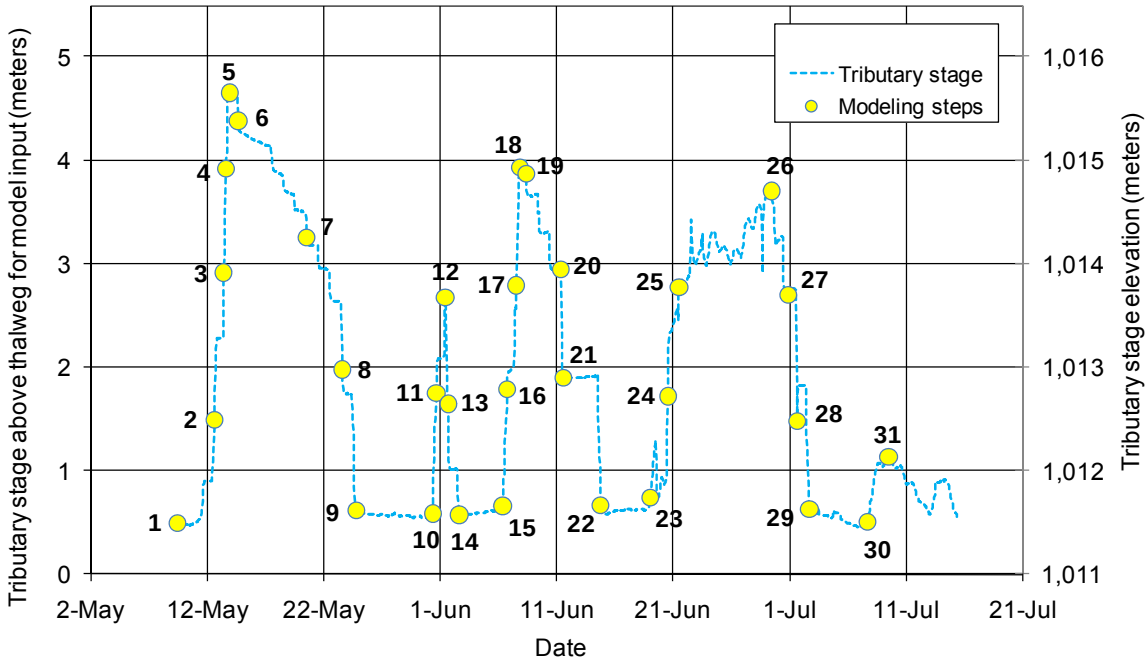

Figure 13. Plot showing the differentiation of the tributary stage into 31 steps for use in modeling Scenarios 1A and 1B. The primary y-axis (left side) represents the tributary stage above the thawleg, which, per the requirements of the BSTEM model, is set to an elevation of zero. The secondary y-axis (right side) represents the real elevations. Steps, or computational nodes, evaluated with the model are numbered and their points are shown in yellow.

The pore-water pressure values recorded at tensiometers A30, A100, and A150 were applied to the three top bank layers. Pore-water pressures for the two bottom bank layers were derived from extrapolation using the values in the above layers. This was achieved by taking the linear relationship between the three upper layers and projecting pore-water pressure values at the mean depths of the two lower layers. For each step, it was confirmed that the sign of a projected pore-

water pressure value in a given layer was in general agreement with the estimated water table elevation within the overall bank profile. Pore-water pressure data from the B-row of tensiometers were not used in the model because these instruments served as a redundant measure in case any of the equally-sized A-row tensiometers failed (which did not occur).

The main objective of these runs was to evaluate whether the model could predict the net conditions actually observed in the field. One element typically considered in bank stability modeling is the erosion of the bank toe material, which we intentionally did not implement in our model runs. We believe that this approach was sound given that the real bank toe in the channel did not erode during the study. Additionally, although BSTEM is capable of modeling toe erosion, it can not successfully do this when the stream stage is directly influenced by flood waters backing up within the modeled channel reach. This is because the model uses the user-entered stream stage and channel slope values to estimate the boundary shear stresses in the channel, which, for this study, would result in an over-prediction of this parameter, leading to high toe erosion rates that are not consistent with our field observations.

The results of Scenarios 1A and 1B are presented in Table 2. The model predicted stable conditions (F_s>1.3) at the study site for every step analyzed, even for Scenario 1B where the bank material cohesion was less due to the absence of vegetation. Because we had not collected pore-water pressures in the two deepest bank layers, we modeled the factor of safety twice in each scenario: once using the field measured pore-water pressures in the bank layers and extrapolating values for the two deepest layers, and once using only the estimated water table, where BSTEM then assigned pore-water pressure values to each layer accordingly. For a given step in each scenario, the F_s values vary depending on whether it is based on the measured or the BSTEM-estimated pore-water pressures; however, the values are still quite similar and, further, none reach the "conditionally stable" (1<F_s<1.3) or "unstable" (F_s<1) thresholds. The F_s values modeled under Scenario 1B are understandably lower than those in Scenario 1A for a given step, which is due to a reduction in cohesion from the absence of vegetation.

Table 2. Model inputs and factor of safety results for Scenarios 1A and 1B.

Step	River discharge at step [A] (cfs)	Tributary stage above the thalweg [B] (m)	Water Table above the tributary thalweg [B] (m)	Factor of Safety, F_s			
				Scenario 1A – with vegetation (c'=10.3 kPa)		Scenario 1B – without vegetation (c'=7.2 kPa)	
				Using pore-water pressures in each layer [C]	Using water table [D]	Using pore-water pressures in each layer [C]	Using water table [D]
1	100	0.04	1.19	2.41	2.30	2.08	1.97
2	1,580	1.03	0.85	2.35	2.54	2.02	2.20
3	3,610	2.46	1.17	2.81	3.08	2.42	2.68
4	5,820	3.46	2.84	3.33	3.02	2.85	2.54
5	7,220	4.20	4.16	3.3	2.73	3.01	2.44
6	6,270	3.92	3.96	3.07	2.55	2.69	2.17
7	3,820	2.80	2.95	2.63	2.32	2.23	1.92
8	1,510	1.52	2.12	1.94	2.13	1.60	1.79
9	355	0.16	1.64	1.91	2.11	1.59	1.79
10	946	0.13	0.88	2.2	2.41	1.88	2.09
11	1,900	1.30	0.83	2.39	2.62	2.05	2.28
12	2,900	2.22	1.17	2.63	2.91	2.26	2.52
13	772	1.19	1.16	2.23	2.46	1.89	2.12
14	409	0.12	0.96	2.18	2.38	1.86	2.05
15	761	0.20	0.72	2.39	2.48	2.06	2.15
16	1,770	1.33	0.69	2.59	2.69	2.25	2.34
17	3,830	2.33	0.88	2.96	3.12	2.56	2.73
18	5,480	3.48	3.14	2.9	2.82	2.42	2.35
19	4,730	3.41	3.39	2.87	2.55	2.41	2.09
20	1,810	2.49	2.60	2.63	2.32	2.24	1.94
21	1,620	1.45	2.15	2.34	2.09	2.00	1.76
22	391	0.22	1.49	2.08	2.17	1.76	1.85
23	662	0.28	0.83	2.29	2.44	1.96	2.11
24	1,590	1.26	0.91	2.46	2.58	2.12	2.23
25	3,260	2.32	1.81	2.93	2.64	2.54	2.26
26	4,620	3.25	3.05	2.88	2.64	2.43	2.19
27	2,880	2.24	2.35	2.59	2.31	2.22	1.95
28	1,560	1.02	2.09	2.24	2.01	1.91	1.69
29	391	0.18	1.58	1.93	2.14	1.62	1.82
30	477	0.06	0.85	2.39	2.42	2.07	2.09
31	896	0.68	0.66	2.50	2.54	2.17	2.21

[A] Discharge measured in the Tuolumne River at the corresponding time step (USGS 11276500).
[B] Height above the channel thalweg, which is set to 0 m in elevation in BSTEM.
[C] Pore-water pressures in the top three layers were from field measured data; pressures in the bottom two layers were estimated based on a projection of the pressures from the layers above.
[D] Water table derived from the deepest tensiometer data, A150; BSTEM calculated pore-water pressures in each of the five bank layers using the water table value.

3.2.2 Scenarios 2A and 2B: threshold of failure identification

Under these scenarios, the threshold of failure was investigated by placing the water table well above the tributary stage, thereby creating a state of high pore-water pressures and internal load. This was accomplished with BSTEM by maintaining a maximum water-table elevation at the bank top while incrementally lowering the tributary stage from this elevation down to the channel bed. For each of these steps, F_s was estimated for both scenarios (Table 3). The results for Scenario 2A indicate that the banks would not become "unstable" at any time but would become "conditionally stable" when the tributary stage is more than 2.0 m below the water table. In Scenario 2B, the lack of vegetation-provided cohesion would result in relatively lower F_s values for a given drawdown step. The banks would become "unstable" when the tributary stage is more than 2.1 m below the water table.

Table 3. Model inputs and factor of safety results for Scenarios 2A and 2B.

Tributary stage above the thalweg [A] (m)	Water table above the tributary thalweg [A] (m)	Factor of Safety, F_s	
		Scenario 2A – with vegetation [B] (c'=10.3 kPa)	Scenario 2B – without vegetation [B] (c'=7.2 kPa)
4.14	4.14	3.28	3.00
3.6	4.14	2.53	2.04
3.2	4.14	2.05	1.62
2.8	4.14	1.72	1.34
2.4	4.14	1.48	*1.13*
2	4.14	1.31	**0.98**
1.6	4.14	*1.19*	**0.88**
1.2	4.14	*1.10*	**0.78**
0.8	4.14	*1.05*	
0.4	4.14	*1.01*	
0	4.14	*1.01*	

[A] Distance above the channel thalweg, as entered into BSTEM.
[B] Values indicating "conditionally stable" conditions ($1<F_s<1.3$) are shown in italics; values indicating mass failure ($F_s<1$) are shown in bold.

3.2.3 Scenarios 3A and 3B: pre-2010 drawdown rates

The final scenarios evaluated with BSTEM entailed calculating the F_s at various steps of drawdown ramping rates implemented in previous years. Prior to 2010, the dam-controlled high-flow releases in spring consisted of relatively faster drawdown ramping rates that generally followed a reduction in river flow by 50% over 4 hours. In this scenario, we co-varied the water table with the falling tributary stage, starting from the bank top. The rate at which the water table lowered with the tributary stage was based on the hydraulic properties of the bank materials. As discussed above, the water table was found to lower in sync with the falling tributary stage when above the threshold elevation of approximately 1,013.5 m. Below this threshold elevation, the water table was found to lower at a reduced rate, which we estimated to be half of the tributary stage lowering rate based on a review of the NPS' well and stage recorder data (Figure 14).

The results of this analysis reveal that the banks would remain "stable" throughout the drawdown periods under both scenarios, although the degree of stability does diminish, reaching a minimum near when the tributary stage is the farthest below the water table (Table 4).

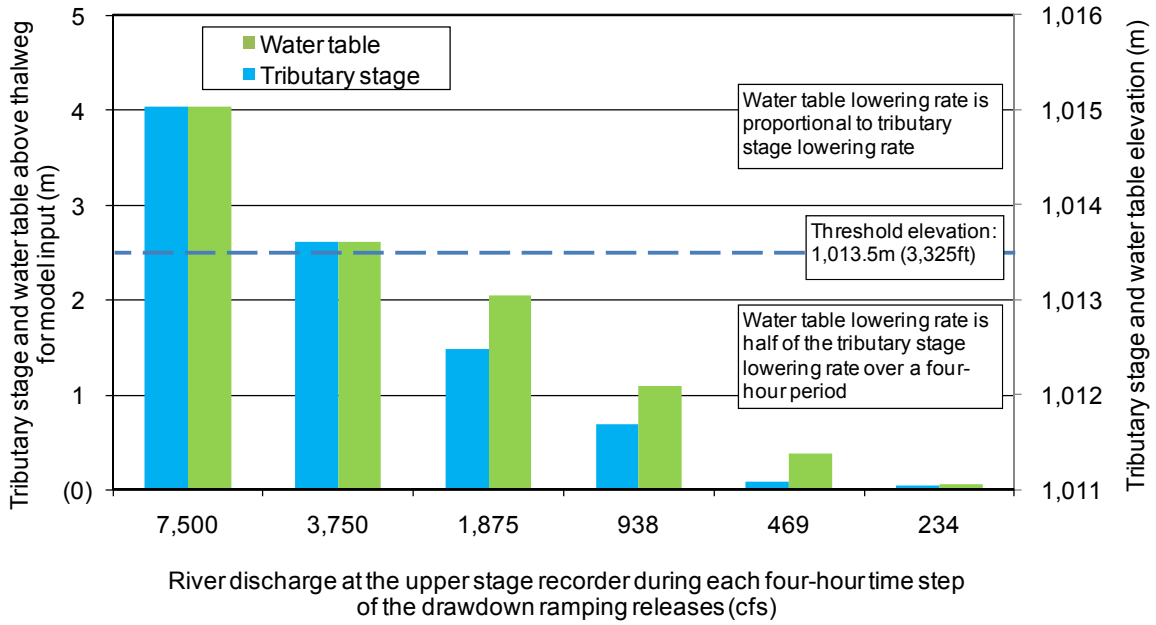

Figure 14. Plot of the tributary stage and estimated water table elevations during drawdown ramping rates as evaluated under Scenarios 3A and 3B. The ramping rates consisted of a 50% reduction of river flow every four hours.

Table 4. Model inputs and factor of safety results for Scenarios 3A and 3B.

Ramping rate time step (hrs)	River discharge at drawdown ramping step [A] (cfs)	Tributary stage above the thalweg [A] (m)	Water table above the tributary thalweg [A] (m)	Factor of Safety, F_s	
				Scenario 3A – with vegetation (c'=10.3 kPa)	Scenario 3B – without vegetation (c'=7.2 kPa)
0	7,500	4.14	4.14	3.26	2.65
4	3,750	2.71	2.71	2.64	2.22
8	1,875	1.59	2.15	2.32	1.96
12	938	0.79	1.19	2.52	2.18
16	469	0.19	0.49	2.73	2.38
20	234	0.00	0.02	2.91	2.55

[A] Distance above the channel thalweg, as entered into BSTEM.

3.3 Bed Mobility Analysis Results

The results of our bed mobility analysis reveal that there is potential for mobilization of all considered particle sizes (D_{50}=2, 10, 20, and 32 mm) under each of the three bed slope scenarios below bankfull stage (Table 5). Given that the bed slope at the study site is about 1%, the corresponding range of threshold flow depths to initiate transport of sands (D_{50}=2 mm) to coarse gravels (D_{50}=32 mm) is about 0.2 to 2.5 m (0.7 ft to 8.2 ft), respectively.

The next step in this analysis was to then compare our predicted incipient motion estimates against measured flow depths in the tributary in order to evaluate whether flows with the potential to mobilize the bed have actually occurred in recent years. This process utilized the Southwest Tributary stage recorder data that NPS staff have been operating since October 2007. For each bed slope scenario in our analysis, Figure 15 shows the measured stage data (adjusted to our study site elevation) overlain with the threshold flow depths necessary to initiate transport of the specific particle sizes. Considering just the 1% bed slope scenario, which is more appropriate for our study site, a key result is that flows in this tributary have been sufficiently high during the past three winters (February-March) to mobilize sand and fine gravel particles (D_{50}≈2 mm), but not high enough to mobilize coarser particles (D_{50}=32 mm). Locally, reaches with similar channel geometries but with steeper bed slopes, such as 4%, could have potentially mobilized fine to medium gravel particles (D_{50}≤10 mm) during these higher flow periods. Conversely, if a lower bed slope is assumed (e.g., S=0.005), then no transport of any particle sizes was estimated due to insufficient shear stresses. Overall, these results suggest that bedload transport is likely an active process in the Southwest Tributary during higher flow periods (e.g., February-March) when river flows are low. This is supported by our field observations of some apparently active gravel bars in the tributary channel.

Table 5. Bed mobility analysis results for four different median particle sizes and three different channel slopes.

Critical shear stress scenario	Calculated critical shear stress, τ_{crit} (Pa)	Calculated critical flow depth for each shear stress and channel bed slope scenario combination (m)		
		S=0.005	S=0.0125 [A]	S=0.04
τ_{crit} (D_{50} =2 mm) [A]	1.5	1.9	0.2	<0.1
τ_{crit} (D_{50} =10 mm)	7.6	2.4	2.0	<0.1
τ_{crit} (D_{50} =20 mm)	15.2	3.1	2.3	<0.1
τ_{crit} (D_{50} =32 mm)	24.3	n/a	2.5	0.1

[A] Most representative of channel conditions at the bank stability study site.

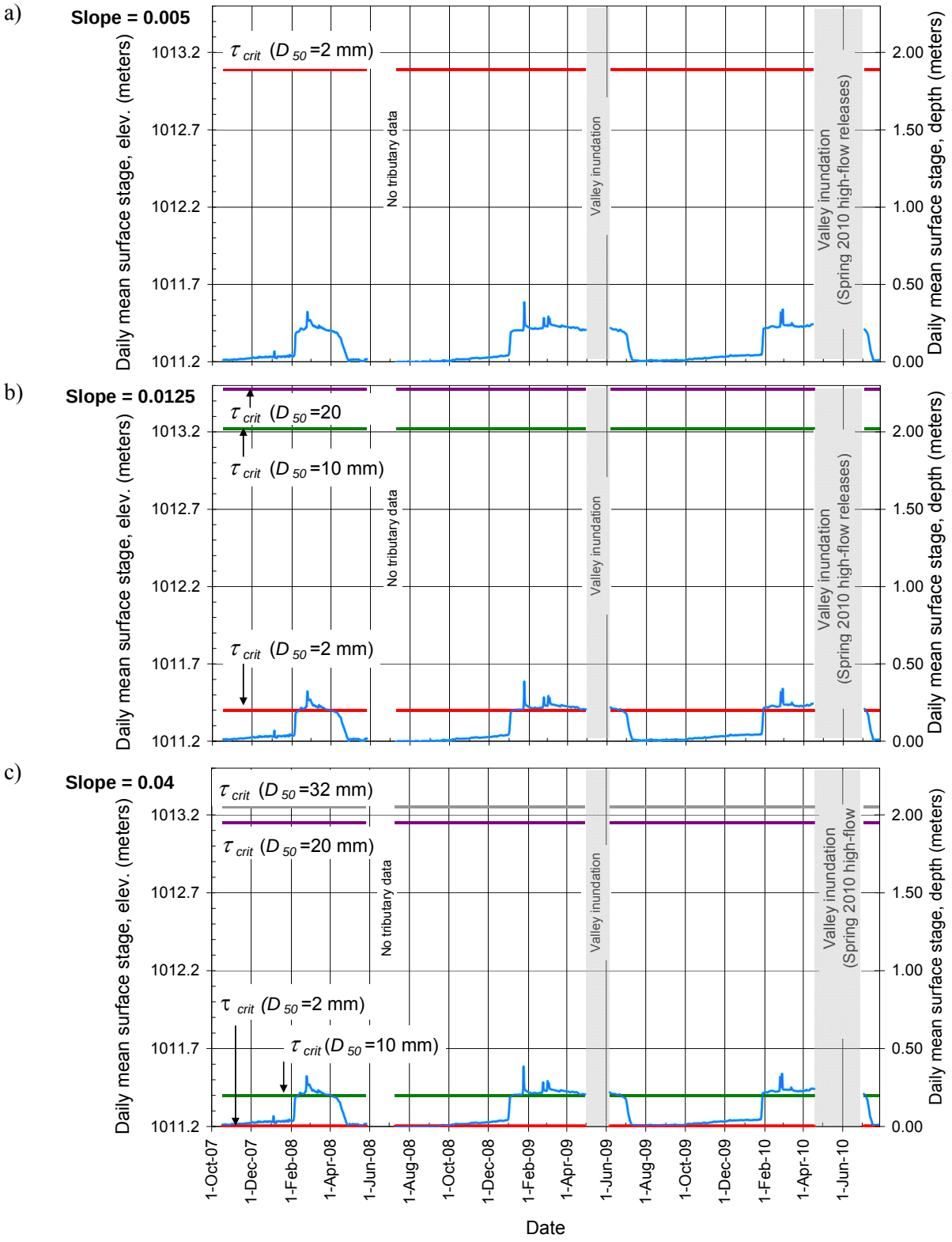

Figure 15. Plot of the bed mobility analysis results showing stage (blue line) at the bank stability study site over time against the threshold stage to initiate bedload transport for four different particle sizes; transport initiates when the stage is greater than the threshold line. Three scenarios with varying bed slope are provided: *S*=0.005 (a), *S*=0.0125 (b), and *S*=0.04 (c).

4 CONCLUSIONS AND RECOMMENDATIONS

This study examined the processes affecting bank stability during three dam-controlled high-flow releases in Spring 2010. The hypothesis going into this study was that bank failures in the valley's tributary channels may be triggered when the drawdown ramping rates were too fast, creating a condition where groundwater levels were not able to drop as quickly as the stream stage. Based on our observations and measurements made during the high flow releases, no mass failures occurred at the study site and only one small failure was triggered along the entire reach of the Southwest Tributary. NPS staff did not note any apparent bank failures along the other two valley tributaries (although these channels were not examined as closely as was the Southwest Tributary). Results of our bank stability modeling predicted that the banks at the study site would be stable during the Spring 2010 high-flow releases. Overall, the stability appears to be maintained through a combination of quickly draining soils in the banks and a dense vegetation cover adding cohesion to the soils. The permeable soils allowed the water table to closely keep pace with the fluctuating tributary stage, thereby limiting the time high pore-water pressures and internal loading were present. An exception occurred when the water table and tributary stage elevations had together fallen about halfway down the bank height, at which point the water table continued to fall, but at a reduced rate. It was during these moments that the model predicted the lowest, albeit still stable, Factor of Safety values.

Modeling of two sets of scenarios of drawdown rates more rapid than those that occurred during the Spring 2010 high-flow releases revealed that the streambanks could potentially become unstable when the water table is considerably higher than the tributary stage and vegetation cover is absent. However, our analysis of the hydraulic conductivity of the bank soils finds that the conditions that were modeled under Scenarios 2A and 2B are not realistic and therefore only the results of Scenarios 1 and 3 are worthy of further consideration here. The results of modeling Scenario 3A and 3B indicate that the standard drawdown ramping rates (i.e., 50% reduction in river discharge every four hours) would likely not induce bank failure in the tributaries, provided the stability of the banks has not been previously reduced by other external forces.

Therefore, based on these results, the primary conclusion of this study is that bank failures in the valley's tributaries do not appear to be adversely affected by the drawdown ramping rates controlled by the dam. It should be noted, however, that these findings are based on one season of data and that continued monitoring of the banks, particularly right before and after future spring high-flow releases, is recommended to confirm the results of this study.

One major control on bank stability not explicitly assessed with the model was lateral scouring of the bank toe and/or vertical scouring of the channel bed by high tributary flows, which can be a primary trigger for the mass failure of a bank. Although neither process occurred at the study site or elsewhere along the tributary channel during the study period, scouring of the bank toe during winter floods has undoubtedly occurred in the past and will occur again in the future. We therefore posit that bank toe erosion processes may play a significant role in the overall stability of the streambanks. In an attempt to provide a first-order assessment of this issue, we performed a cursory sediment transport threshold analysis to gauge the potential of channel bed mobility during recorded flows in the Southwest Tributary when the Tuolumne River flows were low. We estimated that finer bedload particles (e.g., sands and fine gravels) could have potentially been mobilized along the channel bed during the past three winter high flows before the spring high flows (and valley flooding) occurred.

Although the bed mobilization analysis provides some insight into the potential for channel incision and/or erosion of bank toe materials, the overall evaluation is limited in three key respects: (1) the exact hydraulic conditions (e.g., flow velocity and shear stress) at the study site over the assessed time period (October 2007 to July 2010) were not known; (2) the dynamics of bedload discharge (local sediment budget) through the entire tributary channel are not known; and (3) the long-term morphologic trends of the channel are not known. Having hydraulic data to address the first limitation would have allowed for a more robust analysis of the potential for channel bed mobility and/or bank toe scour, which together would have provided greater insight into the active bank failure processes. Regarding the second factor, understanding whether the flux of bed material load through the entire channel is in equilibrium would allow us to better evaluate whether mobilization of bed materials at our study site is indicative of channel stability (i.e., eroded bed sediments are replaced from upstream sources) or channel instability (i.e., eroded bed sediments are replaced from upstream sources at a lower rate than that transported). Finally, understanding the long-term evolution of the channel's morphology, in terms of changes in bed elevation and lateral position, would provide more definitive evidence for channel stability or instability, from which links to primary controls may be discovered when utilizing the results of this study.

In consideration of the findings of this bank stability study and the identified key information gaps, we recommend considering the following additional studies to achieve a more comprehensive understanding of the forces, both resisting and driving, affecting streambank stability and overall tributary evolution in Poopenaut Valley. Firstly, a review of the stream channel morphology and active processes in the valley prior to the construction of O'Shaughnessy Dam should be undertaken in order to compare with present-day conditions and identify the specific changes that have taken place. This type of assessment would ideally allow interested parties to answer vital questions related to the long-term trends in channel migration and incision, and to other changes in the valley, such as land use and vegetation coverage. Our second recommendation relates to the hypothesis that tributary incision and associated bank failure in the valley may either be a natural feature of the valley or driven by the disruption in the synchronicity of flood timing in the river and in the tributaries. The latter hypothesis states that dam operations have shifted the river flooding period forward into spring out of phase with the tributaries, such that bed and bank toe scour occurs when the tributaries are flooding but the mainstem is not. Our limited bed mobilization analysis conducted as part of this study estimated that tributary flows in recent years had the potential to mobilize bed materials, and possibly incise the channel bed, but additional hydrologic information is needed to address the latter hypothesis. An evaluation of historical and contemporary (i.e., pre-dam and post-dam) hydrologic conditions in the mainstem Tuolumne River, along with continuous water stage data in the three tributaries collected by NPS staff, are part of the flow recommendation process that will be summarized in a separate report. Pending the findings of this evaluation and in the case where the latter hypothesis is confirmed, we recommend that the bank stability and bed mobilization analysis be re-visited in the near future after additional years of river and tributary stage data have been collected and are available for use. Furthermore, we recommend that a stage-discharge rating curve be established at each of the tributary water stage recorders to provide vital baseline hydrologic information that would greatly aid future hydraulic and/or sediment transport analyses.

5 REFERENCES

Bear, J. 1988. Dynamics of fluids in porous media. Dover Publications, Mineola, New York.

CDF FRAP (California Department of Forestry and Fire, Fire and Resource Assessment Program). 2010. Statewide fire history electronic database. Website. http://frap.cdf.ca.gov/data/frapgisdata/download.asp?rec=fire [Accessed 25 May 2010].

Domenico, P. A. and F. W. Schwartz. 1998. Physical and chemical hydrogeology. John Wiley and Sons, New York, New York.

Fox, G. A., G. V. Wilson, A. Simon, E. J. Langendoen, O. Akay, and J. W. Fuchs. 2007. Measuring streambank erosion due to ground water seepage: correlation to bank pore water pressure, precipitation and stream stage. Earth Surface Processes and Landforms 32: 1558-1573.

Langendoen, E. J., A. Simon, A. Curini, and C. V. Alonso. 1999. Field validation of an improved process-based model for streambank stability analysis. *In* R. Walton and R. E. Nece, editors. Proceedings 1999 International Water Resources Engineering Conference, Seattle, WA.

Pollen, N. and A. Simon. 2005. Estimating the mechanical effects of riparian vegetation on streambank stability using a fiber bundle model. Water Resources Research 41: W07025. DOI: 10.1029/2004WR003801.

Rinaldi, M., N. Casagli, S. Daporto, and A. Gargin. 2004. Monitoring and modeling pore water pressure changes and riverbank stability during flow events. Earth Surface Processes and Landforms 29: 237–254.

RMC Water and Environment, McBain and Trush. 2006. Upper Tuolumne River: available data sources, field work plan, and initial hydrology analysis. Final report.

Roche, J. 2010. Hydrologist, Yosemite National Park, Resources Management and Science Division. Personal communication with G. Leverich, Stillwater Sciences, providing information on field observations made during and following the Spring 2010 high flow releases.

Sarsby, R. 2000. Environmental geotechnics. Thomas Telford Publishing, London, England.

Simon, A. Geologist, USDA, National Sedimentation Laboratory, Watershed Physical Processes Research Unit Park. Personal communication with G. Leverich, Stillwater Sciences, providing information on the bank stability model, BSTEM.

Simon, A., A. Curini A, S. E. Darby, and E. J. Langendoen. 2000. Bank and near bank processes in an incised channel. Geomorphology 35: 193–217.

Simon, A., R. E. Thomas, A. Curini, and N. Bankhead. 2009. Bank-stability and toe erosion model (BSTEM), static version 5.2. U.S. Department of Agriculture, National Sedimentation Laboratory, Watershed Physical Processes Research Unit. Oxford, Mississippi. http://www.ars.usda.gov/Research/docs.htm?docid=5044

Stock, G., J. Roche, M. Buhler, S. Stock, D. Della-Santina, L. Clor, J. Holmquist, and J. Schmidt-Gengenbach. 2007. Looking downstream: ecological responses to an altered hydrologic regime downstream of Hetch Hetchy Reservoir, Yosemite National Park. Department of the Interior, Yosemite National Park, Division of Resources, Mangement, and Science. April.

Thorne, C. R. 1990. Effects of vegetation on riverbank erosion and stability. Pages 125-144 *in* J. B. Thornes, editor. Vegetation and Erosion. John Wiley and Sons, Chichester, England.